PCCP

PAPER

View Article Online
View Journal | View Issue

Cite this: *Phys. Chem. Chem. Phys.*, 2015, **17**, 5441

Towards a new FRET system *via* combination of pyrene and perylene bisimide: synthesis, self-assembly and fluorescence behavior†

Gang Wang, Xingmao Chang, Junxia Peng, Kaiqiang Liu, Keru Zhao, Chunmeng Yu and Yu Fang*

Received 24th October 2014,
Accepted 13th January 2015

DOI: 10.1039/c4cp04860a

www.rsc.org/pccp

A new fluorescent derivative of cholesterol, *N*,*N*′-(*N*-(2-(3β-cholest-5-en-3yl-formamido)ethyl) pyrene-1-sulfonamido)ethyl perylene-3,4:9,10-tetracarboxylic acid bisimide (CPPBI), was designed and synthesized. In the design, pyrene (Py) and perylene bisimide (PBI) were specially chosen as the energy donor and the acceptor, respectively. Fluorescence studies revealed that (1) CPPBI shows a strong tendency to form supra-molecular assemblies, (2) the assemblies possess a high efficiency of fluorescence resonance energy transfer (FRET) *via* intermolecular interactions, and (3) the profile and position of its fluorescence emission are highly dependent upon the nature of its medium, but the medium shows little effect on the efficiency of the energy transfer, suggesting that the chromophores including both Py and PBI units enjoy some rotational and/or translational mobility in the aggregated state of the compound. Temperature- and concentration-dependent ^{1}H NMR spectroscopy studies revealed that both hydrogen-bonding and π–π stacking play a great role in stabilizing the assemblies of the compound, and confirmed the existence of π–π stacking between the Py moieties and between the PBI residues of the compound, of which the donor and the acceptor may have arranged in an appropriate orientation and at a suitable distance which are the key factors to determine the FRET efficiency. Moreover, the CPPBI-based film possesses unusual photochemical stability, and its emission is sensitive to the presence of some organic vapors, in particular aniline.

Introduction

As an important photophysical technique, fluorescence resonance energy transfer (FRET) has been widely employed for the interrogation of biological problems and for the creation of important functional molecular devices in materials science, such as monitoring protein–protein interactions,[1] study of conformational changes of proteins and other macromolecules,[2–5] detection of particle assembly,[6] construction of fluorescent sensors,[7,8] light-emitting diodes,[9] and light-harvesting molecular systems,[10,11] *etc.* One of the strategies to create a functional object at the molecular level is to integrate a pair of chromophores functioning as donor and acceptor into a single molecule, and this kind of effort has attracted considerable attention during the last few years.[12–17] Harriman *et al.* have synthesized cascade-type Bodipy dyes linked to two aromatic polycycles *via* the boron center that display extremely efficient intramolecular energy transfer.[18] In the artificial light-harvesting system reported by Hariharan and coworkers, naphthalenimide and perylenimide are in an orthogonal arrangement separated by a single bond, of which there is a near-quantitative energy transfer even in the dyad-based metastable vesicular gel.[19–21] It is well known that the efficiency of a FRET process is mainly dependent on the extent of spectral overlap between the emission spectrum of the donor and the absorption spectrum of the acceptor, and the relative orientation of the donor and the acceptor transition dipoles, and furthermore, the efficiency is extremely sensitive to the distance between them.[22–24] Clearly, the creation of FRET systems can be taken as an important strategy to develop new fluorescent probes or sensory materials, of which molecules containing both a fluorescent donor and a fluorescent acceptor may possess superior properties.

In recent years, perylene bisimides (PBIs) are not only used as building blocks for constructing well-defined supramolecular structures due to their unique π–π stacking,[25–33] but are also recognized as excellent candidates for the creation of novel

Key Laboratory of Applied Surface and Colloid Chemistry, Ministry of Education, School of Chemistry and Chemical Engineering, Shaanxi Normal University, Xi'an 710062, P. R. China. E-mail: yfang@snnu.edu.cn; Fax: +86-29-81530787; Tel: +86-29-81530786

† Electronic supplementary information (ESI) available: The synthetic procedures, the characterization data, UV-Vis absorption spectra, some fluorescence spectra, lifetime spectra of the compound, AFM image, fluorescence spectra of the sensing film and the Förster distance R_0 for FRET. See DOI: 10.1039/c4cp04860a

optoelectronic materials[34–37] and fluorescent sensors[38–41] because of their exceptional stability and outstanding optical properties. In addition, the imide substituent has a negligible influence on the absorption and emission properties of PBIs.[42] Therefore, to design and synthesize functional molecules based on PBI, introducing substituents at the imide nitrogen is one suitable method to improve its performance in applications, in particular as an energy acceptor. Würthner and colleagues designed and fabricated a series of energy transfer systems by using PBI as an energy acceptor, of which some exhibit remarkable color-tunable luminescence, even white-light, tuned by aggregation.[7,43]

For creating an energy donor–acceptor system, it is extremely important to choose a suitable donor–acceptor pair as the spectral overlap between them plays a great role in the efficiency of the relevant FRET process. As it is well known, as a fluorophore, pyrene (Py) has a number of advantages such as a long singlet lifetime, sensitive to the changes of the polarity of its micro-environment, a strong tendency to form an excimer which possesses high fluorescence quantum yield, as well as a broad and structure-less emission centering at 480–500 nm,[44–46] which is totally covered by the absorption spectrum of PBI. Accordingly, Py and PBI may be taken as an ideal pair of donor and acceptor.

Based upon these considerations, a new FRET system was purposely designed and synthesized. In the design, the PBI unit was put in the center, and two Py units and two cholesteryl moieties were introduced through diethylenetriamine (CPPBI). The detailed structure of the compound is shown in Scheme 1. The cholesteryl unit was introduced in order to adjust the self-assembly property and improve the solubility of the compound in organic solvents.[41,47,48] The synthesis route towards the compound is shown in Scheme S1 (ESI†). It was expected that the target compound may be applied to chemical sensing, and the Stokes shift of it should be significantly enlarged when compared to that of PBI or Py because of possible FRET from the Py unit to the PBI structure. As it is known, large Stokes shift must be beneficial to avoid interference of the excitation light with the measurement of the fluorescence emission, a favourable factor for creating the compound-based sensing devices. This paper reports the details of the synthesis and the fluorescence studies of the compound.

Experimental

Reagents and materials

Pyrenesulfonyl chloride (PSC) was synthesized according to a literature method.[49] PTCDI-Chol with 1,3-propanediamine as the linker between the cholesteryl and the PBI units was synthesized according to a literature method.[41] Di-ethylenetriamine (Sigma-Aldrich, >99.0%), cholesteryl chloroformate (Alfa Aesar, >98.0%), *tert*-butyl phenyl carbonate (Sigma-Aldrich, >98.0%), and 3,4:9,10-perylenetetracarboxylic dianhydride (J&K Chemicals, >98.0%) were used directly without further purification. Zinc acetate was obtained by the thermal dehydration of zinc acetate dihydrate. Except where specified otherwise, all other reagents were of analytical grade and used without further purification or treatment. All organic liquids were of analytical grade. Water used in this work was acquired from a Milli-Q reference system.

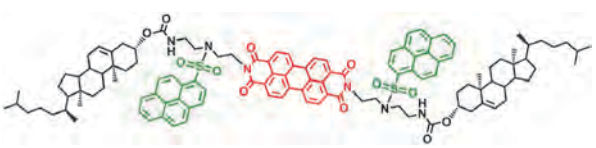

Scheme 1 Molecular structure of the compound (CPPBI).

Measurements

All samples used for absorption and fluorescence spectra measurements were prepared in a quartz cell with side length 1 cm. Before each measurement, the samples were thoroughly de-gassed by bubbling argon at room temperature for more than 30 min. UV-Vis absorption spectra were recorded on a U-3900 UV-Vis spectrophotometer (Hitachi) at a concentration ranging from 1.4×10^{-5} mol L^{-1} to 4.0×10^{-6} mol L^{-1} in chloroform. Steady-state fluorescence excitation and emission spectra were obtained by using a time-correlated single photon counting fluorescence spectrometer (Edinburgh Instruments FLS920) with xenon light at room temperature except temperature-dependent emission measurements. Cut-off filters may be used to eliminate scattered light during the measurement of relevant fluorescence excitation and emission spectra. Absolute fluorescence quantum yields were determined on the same system using the integrating sphere method. Lifetime and time-resolved emission spectra (TRES) were measured on the same system using an EPL-375 picosecond pulsed diode laser with vertical polarization (70.3 ps pulse width) as an excitation source at a concentration of 1.0×10^{-6} mol L^{-1} in chloroform. The wavelength range of the TRES measurements was maintained from 395 nm to 743 nm. The monochromator was driven in a 3 nm step under the control of a computer. The accumulation time for each decay curve (a specific $\lambda_{ex}/\lambda_{em}$) was 120 s. For the ^{1}H NMR study, the sample containing the as-obtained compound and $CDCl_3$ was prepared in a NMR tube, and the chemical shifts were determined by using a Fourier digital NMR spectrometer (Bruker Avance, 300 MHz) at a given temperature between 298 K and 318 K or at a given concentration ranging from 2.6×10^{-3} mol L^{-1} to 10.4×10^{-3} mol L^{-1}. The ^{1}H NMR spectra and the chemical shift correlation spectroscopy (COSY) spectrum of CPPBI were recorded on a Bruker Avance 600/400 NMR spectrometer. The MS were collected on a Bruker maxis UHR-TOF mass spectrometer in ESI positive mode and MADI-TOF mode by using α-cyano-4-hydroxycinnamic acid (CCA) and dithranol as the matrixes. The FTIR spectra were measured on a Fourier transform infrared spectrometer (Vertex 70v, Bruker, Germany). Melting point measurements were conducted on an X-5 microscopic melting point meter (Beijing Tech Instrument). Scanning electron microscopy (SEM) pictures of the film were taken on a Quanta 200 scanning electron microscope (Philips-FEI) at an accelerating voltage of 25 kV. Transmission electron microscopy (TEM) image was obtained using a JEOL JEM-2100 transmission electron microscope at an acceleration voltage of 200 kV.

Samples for TEM measurements were prepared by immerging a pure carbon-coated copper grid into the chloroform solution of CPPBI (1.0×10^{-6} mol L^{-1}), and then the copper grid was removed out from the solution and the solvent on its surface was evaporated completely at room temperature. Typical tapping-mode atomic force microscopy (AFM) measurements were finally conducted by using a CSPM 5500 scanning probe microscope (Being Nano-Instruments, Ltd, Guangzhou, China). The sample for AFM measurements was prepared by dip-coating the chloroform solution of CPPBI (1.0×10^{-6} mol L^{-1}) onto a freshly cleaved mica surface and allowing it to dry in air.

Fabrication of the CPPBI-based film

Self-assembly of CPPBI into aggregates was performed by a rapid solvent-dispersion process.[50] For a typical preparation, 1.7 mg of CPPBI was added to 1360 μL of chloroform in a centrifuge tube, and then 2040 μL of *n*-propanol was rapidly added to the CPPBI solution. The final concentration of the compound was 2.6×10^{-4} mol L^{-1} and the volume ratio of chloroform to *n*-propanol was 2 : 3, which is the best experimental condition optimized by repeating numerous tests. It is believed that within this system aggregates with suitable morphology, size and dispersiveness form spontaneously. After a while, the mixture was centrifuged at 6500 rpm for 30 min. Then, a defined amount (15 μL) of the as-prepared solution (upper part) was dip-coated on a glass substrate which was pre-treated with a "piranha solution" (30% H_2O_2/98% H_2SO_4, v/v, 3/7) (**Caution:** it must be handled with extreme care) at 98 °C for 1 h and dried in air for 30 minutes at room temperature before the measurement.

Results and discussion

Optical behaviour of CPPBI in solution state

The absorption spectrum of CPPBI dissolved in chloroform presents strong absorption bands around 364 nm ($\varepsilon = 5.2 \times 10^4$ L mol^{-1} cm^{-1}) and around 541 nm ($\varepsilon = 5.1 \times 10^4$ L mol^{-1} cm^{-1}), which can be, as expected, assigned to the characteristic absorption of Py and PBI units, respectively (Fig. S1, ESI†).

As there is a large overlap integral between the broad Py excimer emission centering at 480–500 nm (ref. 45) and the absorption from 460 nm to 600 nm of PBI derivatives (Fig. S2 and S3, ESI†), energy transfer from the Py excimer to PBI may occur under suitable conditions provided they are used as the energy donor and acceptor, respectively. In addition, as reported already,[25–33] PBI derivatives have a strong tendency to form well-organized aggregates *via* π–π stacking, of which the PBI moieties must be arranged at a suitable distance and in a specific orientation. Accordingly, it is highly reasonable to expect that efficient energy transfer may occur within a CPPBI molecule or among different CPPBI molecules. This prediction was confirmed by the fluorescence emission measurements at a concentration of 5.0×10^{-6} mol L^{-1} in chloroform at room temperature as shown in Fig. 1. Reference to the figure reveals that a broad and structure-less emission was clearly observed at 624 nm, of which the position is independent of the excitation wavelength adopted,

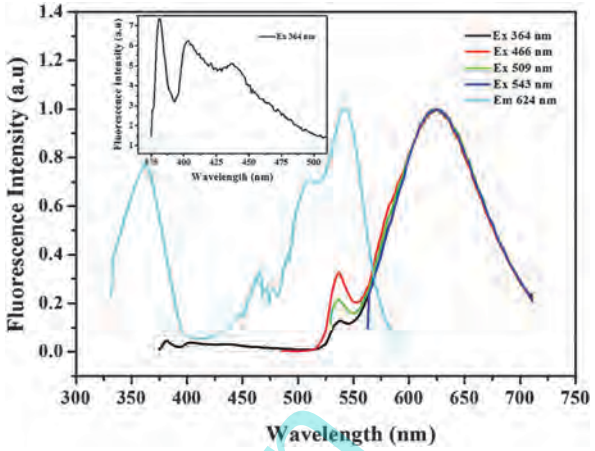

Fig. 1 Normalized fluorescence excitation and emission spectra of CPPBI in chloroform at a concentration of 5.0×10^{-6} mol L^{-1}. The detected wavelength was set at 624 nm, and the excited wavelength was 364, 466, 509, and 543 nm, respectively. The inset is a magnified form of the residual pyrene emission region upon excitation at 364 nm.

and can be definitely attributed to the PBI unit of the compound.[27] On further examination of the spectra shown in the figure, it is seen that accompanying the main emission indicated, a very weak emission within 375–450 nm appears as shown in the inset figure which should originate from the Py structure of the compound when 364 nm, the characteristic excitation wavelength of the Py unit, was adopted as the excitation wavelength where excitation of the PBI unit is negligible (Fig. S4, ESI†), indicating that the excited energy of the donor is successfully transferred to the acceptor, of course *via* an intermediate, the Py excimer. With the exception of the two emissions discussed, a weak emission at 536 nm, the specific emission of PBI in its mono-molecular state,[51] was also observed, and similarly its position is also independent of the excitation wavelength. Furthermore, similar to the UV-Vis absorption spectrum of CPPBI, its fluorescence excitation spectrum monitored at 624 nm also displays several excitation bands, of which one is composed of three peaks which are 466 nm, 509 nm and 543 nm, respectively, and the other appears at 364 nm. With reference to the literature, it is not difficult to assign the excitation band at 466 nm to the electronic transition of S_0–S_2, and the excitation bands at 509 nm and 543 nm to the S_0–S_1 transition of the PBI moieties.[52] As for 364 nm, it is a typical excitation wavelength of the Py unit (Fig. S2, ESI†). Compared to the absorption spectrum of CPEC, a Py derivative, and that of a PBI derivative, PTCDI-Chol (Scheme S2, ESI†) in mono-molecular state as shown in Fig. S2 (ESI†) (the maxima appearing at ~352 nm and ~527 nm, respectively), of which each resembles one part of the CPPBI structure, the corresponding absorption bands of CPPBI in the present case are significantly red-shifted and appear at 364 nm and 541 nm, respectively. These results suggest that the PBI moieties might exist in a stacked state in the system. Furthermore, the fluorescence quantum yields of the PBI moiety and the relevant compounds in the system were determined, and the results are shown in Table S1 (ESI†). With reference to the table, it is found that the PBI moiety of the compound could be effectively excited

or even more efficiently excited at a wavelength of 364 nm, a typical excitation wavelength of the donor, Py unit, suggesting a significant communication between the two moieties.

Concentration effect

Considering the fact that there are two Py moieties in a CPPBI molecule, it is highly possible that the Py excimer, which is a pre-requirement for energy transfer from the Py unit to the PBI moiety of the molecule, could be formed *via* either intramolecular or inter-molecular interaction. To make sure the origin of the intermediate, Py excimer, concentration-dependent fluorescence measurements were performed. During the tests, 364 nm was chosen as the excitation wavelength to selectively excite the Py unit. The concentrations of CPPBI used for the measurements ranged from 1.0×10^{-8} mol L^{-1} to 1.0×10^{-5} mol L^{-1} in its chloroform solution. Some typical results from the measurements are displayed in Fig. 2. It is clearly seen that with the increase in the concentration of CPPBI, the emission at 624 nm, typical emission of PBI, increases significantly, but the emission from Py moieties did not change very much, a typical phenomenon of energy transfer *via* inter-molecular interactions. To find out if the intermolecular interaction could occur at a concentration of 1.0×10^{-8} mol L^{-1}, the emission profile was recorded by increasing the width of the emission slit, and the results are depicted in Fig. S5 (ESI†). It is seen that the emission of the PBI unit is still there, and independent of the excitation wavelength adopted, suggesting that energy transfer *via* intermolecular interaction still takes place at such a low concentration. On further decreasing the concentration to 1.0×10^{-9} mol L^{-1}, however, the emission from PBI disappears, and the excitation spectrum of the system was characterized by Py excitation, as shown in Fig. S6 (ESI†). This result demonstrates clearly that (1) direct excitation of the PBI unit at 364 is negligible, (2) Py excimer formation *via* intramolecular interaction is impossible, a result supported by molecular dynamics modelling as shown in Scheme S3 (ESI†), where the distance between the two Py units is more than 13 Å, which is much larger than that for excimer formation (3.0–3.5 Å), and (3) the energy transfer from Py to PBI takes place *via* intermolecular interaction. It is because that only the excimer emission of the Py moiety of CPPBI well matches the absorption of the PBI unit that the emission of PBI in the present study must depend upon the probability of the formation of Py excimer, and thereby, the increase in PBI emission is reasonably considered to be caused by the increase in the numbers of the Py excimer of the compound due to the increase in its concentration, a result of typical intermolecular interaction.

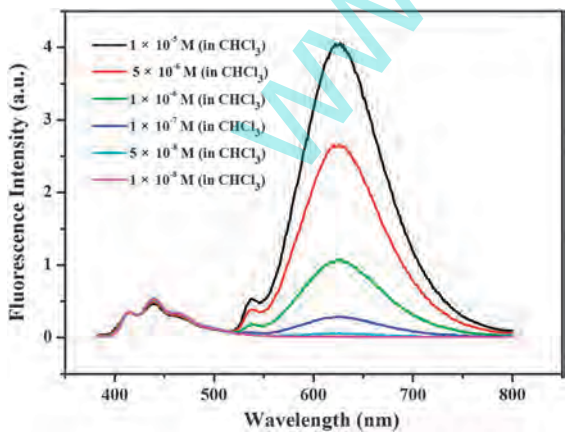

Fig. 2 Concentration-dependent fluorescence emission spectra of CPPBI in chloroform from 1.0×10^{-8} mol L^{-1} to 1.0×10^{-5} mol L^{-1} upon excitation at 364 nm.

The fact that there is no Py excimer emission within the whole concentration range studied as shown in Fig. 2 indicates that energy transfer or electron transfer occurs in the system.[12,14,53,54] It is known that the electron transfer rate (k_{ET}) increases with increasing temperature, and the rate constant (k_{ET}) can be calculated by using eqn (1):

$$k_{ET} = \nu \cdot \exp\left(-\frac{\Delta G^{\neq}}{RT}\right) \quad (1)$$

where R is the gas constant, T the absolute temperature, ν the frequency factor, and $\Delta G^{\neq}$ the Marcus free energy. In contrast, energy transfer *via* Förster mechanism is basically independent of temperature change,[55] and thereby, it is reasonable to determine if electron transfer is significant during the process. As depicted in Fig. S7 (ESI†), the emission of the PBI moiety slightly increases with increasing temperature upon excitation of the Py moiety at 364 nm, suggesting that electron-transfer is negligible and Förster resonance energy transfer (FRET) is the main type of energy transfer in the process. In other words, energy transfer *via* Dexter mechanism (two-electron process) may be excluded. As a result, the reason explaining the fact that excitation at the characteristic excitation wavelength of the Py unit results in increased PBI emission can only be attributed to highly efficient FRET from Py, *via* its excimer, to PBI. A similar result was obtained from another temperature-dependent fluorescence measurement where a wider temperature range was reached because tetrachloroethane, which possesses a higher boiling point, was employed as the solvent (Fig. S8, ESI†). By the way, the characteristic Förster distance, R_0, of this system (35.9 Å) can be calculated, and the details of the calculation can be found in ESI.†

As for the FRET efficiency of the system under study, it can be calculated by using eqn (2):[23]

$$E = 1 - (\tau_{DA}/\tau_{D}) \quad (2)$$

where τ_{DA} and τ_{D} are the relative fluorescence lifetimes of the donor (Py) in the presence of the acceptor (PBI) and that in the absence of the acceptor, data which could be obtained by using the reference compound CPEC as a sample. Accordingly, the τ_{D} of the reference compound was determined at a relatively high concentration. Its average was calculated, and was found to be 18.0 ns (*cf.* Fig. S9, ESI†). The τ_{DA} of the CPPBI system was also determined, and the value is 1.6 ns (Fig. S10 and Table S2, ESI†). As a result, a FRET efficiency of 91% was obtained. The great FRET efficiency can only be rationalized by considering the fact that CPPBI has a strong tendency to form organized supramolecular aggregates in which the orientation and distance of

the Py units are highly favorable for the formation of Py excimers, and furthermore they are very close to the energy acceptor, PBI moieties. Interestingly, the FRET process is so efficient that it takes place at a concentration lower than 1.0×10^{-8} mol L^{-1} even in a good solvent like chloroform (Fig. S5, ESI†), which could be partially attributed to the special design of CPPBI which is the chemical linkage of the donor and the acceptor, as well as the cholesteryl unit, which may enhance the aggregation of the CPPBI molecules *via* the well-known van der Waals interaction. The result of TEM measurements revealed the aggregation of CPPBI in its chloroform solution, and the size varies from 100 nm to 200 nm, as shown in Fig. 3. The aggregation of the compound was further confirmed by AFM measurements (Fig. S11, ESI†).

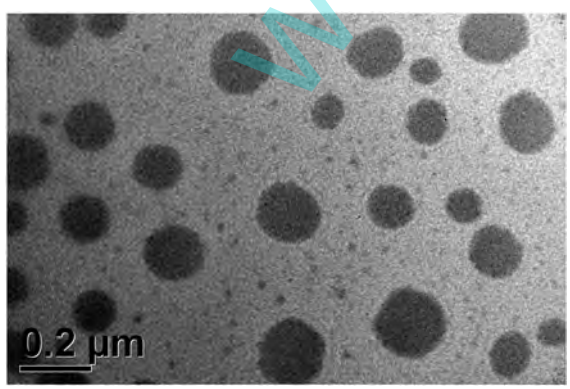

Fig. 3 The TEM image of the aggregated CPPBI from its chloroform solution at a concentration of 1.0×10^{-6} mol L^{-1}.

Solvent effect

The fluorescence emission spectra of CPPBI in a variety of solvents including toluene, benzene, chloroform, *n*-hexane and ethanol were recorded at a concentration of 5.0×10^{-6} mol L^{-1}, and the results are shown in Fig. 4. As aromatic and chlorinated solvents show a strong ability to screen π–π stacking,[42] it should not be difficult to understand why the compound is much easier to be dissolved in toluene, benzene and chloroform. Interestingly, no matter which solvent mentioned above is adopted to prepare CPPBI solution, excitation at 364 nm results in the emission of PBI as always, indicating efficient FRET from the Py moiety to the PBI acceptor (Fig. 4). Further inspection of the emissions shown in the figure reveals that the profile and the position of the emission are highly dependent upon the dissolving ability of the solvent towards the compound. With decreasing dissolving ability, the position of the maximum emission of the PBI structure tends to shift to longer wavelengths and the intensity decreases with it. Furthermore, monomer emission around 536 nm from the PBI unit appears when the compound was dissolved in good solvents such as toluene, benzene, and chloroform. For chloroform, the emission from the aggregated state of PBI shifted to 624 nm. For poor solvents, such as *n*-hexane and ethanol, the emission shifted to an even longer wavelength, 662 nm. It is known that one-dimensional structure formation *via* self-assembly of molecules is a result of

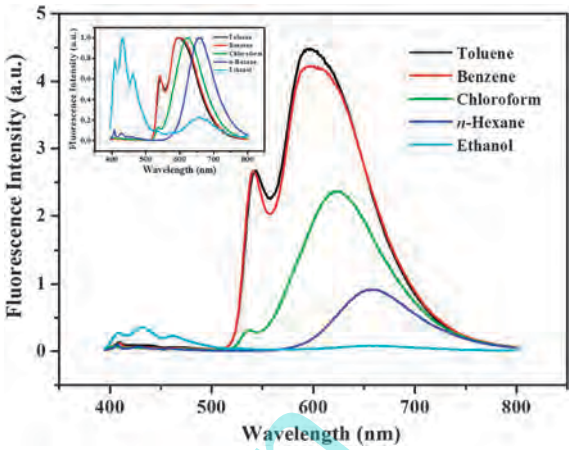

Fig. 4 Fluorescence emission spectra of CPPBI in different solvents (5.0×10^{-6} mol L^{-1}, λ_{ex} = 364 nm). The inset is the normalized fluorescence emission spectra of CPPBI in the solvents (5.0×10^{-6} mol L^{-1}, λ_{ex} = 364 nm).

competition between molecular stacking and dissolution,[50] and thereby screening of π–π stacking favors dissolution of the compound, resulting in smaller aggregates and less red shifted emission. This is a reason that may explain why good solvents favor the formation of mono-PBI unit emission, and in contrast poor solvents favor aggregated-PBI emission. As for the decrease of the emission of the PBI upon decreasing the dissolving ability of the solvent, it could be understood by considering the fact that strong π–π stacking is unfavorable for radiation decay of the excited state of the π systems due to the inner-filtering effect which is directly related to the emission from the aggregates of PBI moieties.

^{1}H NMR studies

NMR spectroscopy is a powerful technique to study supramolecular interactions.[56] Accordingly, to identify which types of interactions lead to the aggregation of CPPBI, temperature-dependent ^{1}H NMR measurements for the solution of CPPBI in $CDCl_3$ were conducted, and a section of ^{1}H NMR spectra for the N–H protons in amide groups and the aromatic protons in Py and PBI structures are shown in Fig. 5(a). It can be seen that at a temperature of 298 K, two doublet peaks of PBI protons appeared at 7.92 and 7.66 ppm, respectively, but the signals shifted to 7.93 and 7.68, respectively, when the temperature was increased to 318 K, which affords noticeable evidence for the existence of π-stacked arrangement of the PBI units. It is to be noted that the assignment of the proton signals was confirmed by ^{1}H–^{1}H chemical shift correlation spectroscopy (COSY) studies, and the details can be found in Fig. S12 (ESI†).

Meanwhile, the signals of Py protons located in the region of 6.77–8.56 ppm with the exception of those belonging to PBI gradually shifted to the downfield along with increasing temperature, indicating interaction among the Py moieties. In contrast, the N–H proton presented a peak at 5.29 ppm at 298 K, but shifted to 5.26 ppm at 318 K, which apparently demonstrates that hydrogen bonding plays a key role in stabilizing the self-assembled structure of the compound. A similar

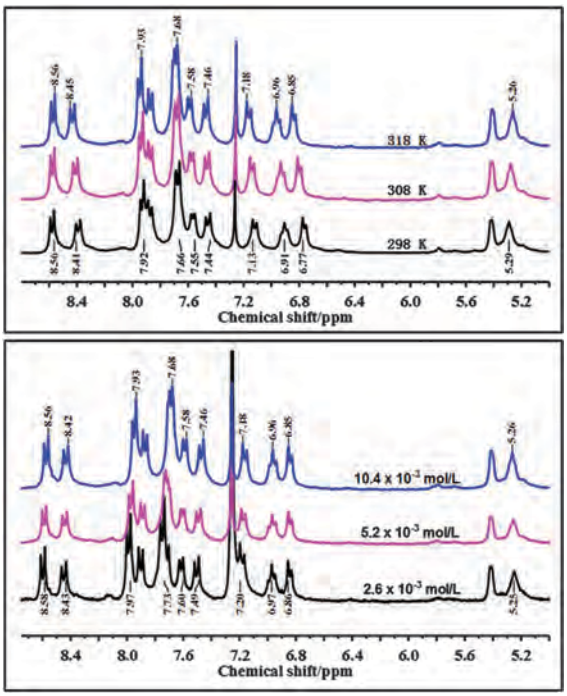

Fig. 5 (a) Temperature-dependent ^{1}H NMR spectra of CPPBI in $CDCl_3$ (top); (b) concentration-dependent ^{1}H NMR spectra of CPPBI in $CDCl_3$ (bottom).

but much more broad change was observed on conducting the temperature-dependent ^{1}H NMR measurement in tetrachloroethane, which possesses a higher boiling point (Fig. S13, ESI†).

To further elucidate whether the hydrogen bonding and π–π stacking belong to intermolecular interaction or intramolecular interaction, additional ^{1}H NMR measurements were performed at 318 K at concentrations ranging from 2.6×10^{-3} mol L^{-1} to 10.4×10^{-3} mol L^{-1}, and the results are shown in Fig. 5(b). It can be clearly observed that the results obtained by decreasing the concentration are similar to those obtained by increasing the temperature, which intensively suggests that the changes in the chemical shift of the N–H protons and that of the aromatic protons may arise from intermolecular π–π stacking and intermolecular hydrogen-bonding.

TRES studies

As described already, for the systems under study, the Py excimer was recognized as the intermediate for the energy transfer from Py to PBI. It is known that the excimer could be formed *via* either the Briks' scheme or a pre-formed scheme.[45,57] The former, however, requires relatively mobile Py moieties so that nearby translational and/or rotational diffusion of them is possible, but for the latter one, ground state dimers of the moieties should exist so that direct excitation of them is possible. In addition, exploration of the origin of the excimer formation is helpful for understanding the details of the self-assembled structures of the compound in the systems. As reported in the literature, the time-resolved emission spectroscopy (TRES) technique is one of the most powerful techniques to distinguish the two schemes for excimer formation of poly-aromatics.[45,58] Accordingly, TRES measurements were conducted at 1.0×10^{-6} mol L^{-1} in chloroform using a picosecond pulsed diode laser (EPL-375) as an excitation source, which is believed to provide us detailed information on the energy transfer process. The results are shown in Fig. 6. It is clearly observed that the emission at longer wavelengths from PBI makes a considerable contribution to the profile of the earliest time gate (0–1 ns) spectrum, which may be caused by two reasons. The first is that the Py units within the aggregates formed a ground state dimer before the excitation pulse, and the dimer is directly excited and transfers its energy to PBI. The other is that the PBI unit is directly excited as a longer excitation wavelength, 375 nm, was adopted. The spectrum taken at the time gate of 5–9 ns is dominated by Py emission, and the contribution from PBI decreases significantly. However, with the time gate moving to even longer times, the spectrum is increasingly dominated by the PBI emission, in particular for the time gate of 18–200 ns. As for the change of the contribution of PBI emission to the TRES spectrum that is high at the earlier time gate, low at the middle time gate, and high again at the later time gate, the finding may be reasonably explained by considering the fact that the PBI unit was excited mainly *via* energy transfer from the two different Py excimers, of which one is

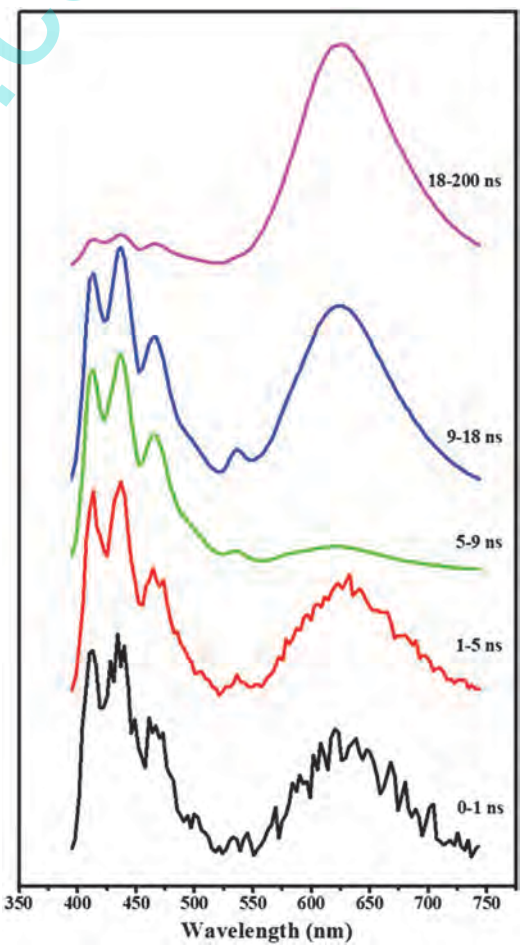

Fig. 6 Time-resolved emission spectra of CPPBI in chloroform at a concentration of 1.0×10^{-6} mol L^{-1}.

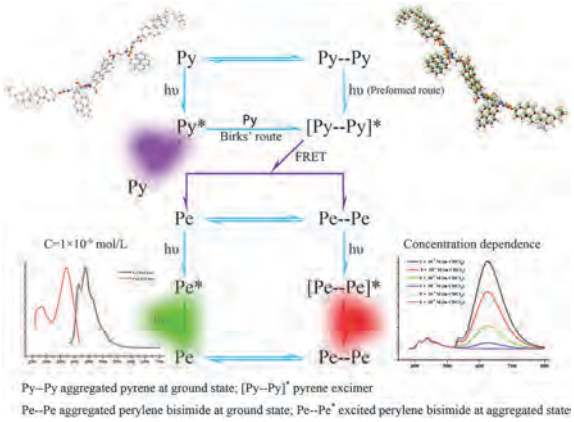

Fig. 7 Schematic representation of the FRET process in a solution of CPPBI in a suitable solvent and at a suitable concentration.

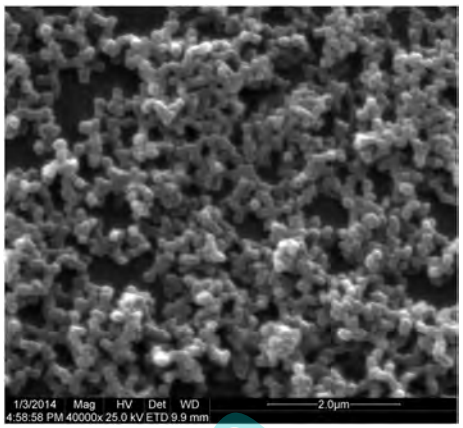

Fig. 8 The scanning electron microscopy image of the sensing film: CPPBI physically coated on a glass plate surface.

formed *via* the pre-formed scheme and the other *via* the Birks' scheme as confirmed by TRES measurements, because the two excimers appear at different times after each light pulse. These results demonstrate that Py moieties in the aggregates exist in π–π stacked states and they are relatively mobile. Furthermore, the π–π stacked Py units are very close to the π–π stacked structures of PBI, which is strong evidence to support the argument that the PBI emission originated mainly from the Py excimer mediated FRET between the Py moieties and the PBI structures in the aggregates of CPPBI. The formation of the Py excimer *via* the two schemes was confirmed by TRES studies of a chloroform solution of a reference compound, CPEC (Fig. S14, ESI†).

On the bases of the steady-state and time-resolved fluorescence studies discussed above, it is believed that the molecules of CPPBI in a suitable solvent and at a reasonable concentration, such as chloroform and at concentrations greater than 1.0×10^{-8} mol L^{-1}, exist in aggregated state, in which the Py moieties are close to each other favoring the formation of the excimer *via* both the Birks' route and the pre-formed route, and furthermore, the PBI units also aggregate with each other. It is the aggregation and the spectral overlap of the Py excimer emission with the excitation of the PBI unit that makes excitation of the system at the Py position emitting at a far red position which is a characteristic of the emission of PBI aggregates. A schematic representation of the FRET process is shown in Fig. 7.

Photochemical stability of the CPPBI-based fluorescent film and its response to organic vapours

The excitation and emission spectra of the as-prepared fluorescent film were measured and the results are depicted in Fig. S15 (ESI†). Reference to the spectra shown in the figure reveals that they are similar to those recorded from the solution sample of the compound at higher concentrations, suggesting that the compound, CPPBI, also exists in an aggregated state in the as-prepared film. The only difference is that the Stokes shift in this case is even larger and reaches 294 nm since the maximum emission appears at 658 nm, and the excitation adopted is 364 nm. SEM studies confirmed the aggregation of CPPBI in the film state as shown in Fig. 8. It is clearly seen that the aggregates are defined spherical particles with an average diameter of around 150 nm, and the particles tend to form networked structures. Furthermore, it is delightful to find that unlike other aromatics-based films,[59] photo-chemically, the film fabricated with CPPBI possesses exceptional stability. As depicted in Fig. S16 (ESI†), 2 hours continuous photo-illumination results in less than 7% deduction of the fluorescence emission of the film, suggesting good stability of the film, which lays foundation for its real-life uses.

It is well known that fluorescent films are commonly used for sensing, and thereby it should be interesting to examine the response of the film to organic vapours. The results are shown in Fig. S17 (ESI†). It is seen that the fluorescence emission of the CPPBI-based film is significantly quenched by the presence of organic amines, in particular aniline, in vapor phase. In contrast, the presence of other commonly found organic liquids such as chloroform, THF and dichloromethane enhances the emission of the film. As for toluene, benzene, acetone, methanol, cyclohexane, *n*-hexane, acetic acid, water, and acetonitrile, as well as electron-deficient nitro-aromatics such as nitromethane, 2,4-dinitrotoluene, *p*-nitro-aniline and nitro-benzene, they show little effect on the emission of the film. For aniline, less than 7 ppb could result in more than 8% deduction of the fluorescence emission of the film (Fig. S18, ESI†). Considering the selectivity, the sensitivity and the exceptional photo-chemical stability, the film fabricated may be developed into a sensor for aniline and/or other organo-amines, which are the markers of lung cancer.[60]

Conclusions

In conclusion, a cholesterol-containing fluorescent compound, CPPBI, with Py and PBI as the main building blocks was designed and synthesized. Fluorescence studies revealed that combination of two Py moieties and one PBI unit into a single molecule using cholesterol as another structural unit resulted in a molecule showing a strong tendency to form ordered and densely stacked supra-molecular assemblies both in solution and in film state. Concentration-dependent fluorescence and TRES studies revealed

that for the compound in solution state, FRET from Py to PBI takes place *via* intermolecular interaction even at a concentration as low as 1.0×10^{-8} mol L^{-1}, which suggests that the fluorescence emission of the CPPBI-based systems is always characterized by emission from PBI, the acceptor of the FRET process. Furthermore, in conjunction with the result from FRET studies, the solvent-dependence of the profile and position of the emission spectrum of CPPBI in solution state shows that the molecules of CPPBI, in particular their core structure, PBI, enjoy some mobility in the aggregated state. This tentative conclusion is further supported by the results from TRES studies, which revealed that the energy transfer intermediate, the Py excimer, may form *via* both the pre-formed scheme and the Birks' scheme, implying that the Py unit possesses some rotational and/or translational mobility. Further studies revealed that photochemically, the CPPBI-based film is super-stable, and sensitive to the presence of some organic liquids in vapor phase, in particular aniline. In contrast, the presence of vapours of electron-deficient compounds and water has little effect on the emission, suggesting that the film may be developed into a fluorescent chemo-sensor for aniline and/or other organo-amines. Temperature-/concentration-dependent ^{1}H NMR spectroscopy studies revealed that inter-molecular hydrogen bonding and π–π stacking are the main driving forces for the formation of aggregates.

Acknowledgements

This work was supported by the Natural Science Foundation of China (21273141), the 111 project, and the Program for Changjiang Scholars and Innovative Research Team in University (IRT1070). Furthermore, Miss Lin Wang and Yalu Guo are thanked for their help in the synthesis of the compound and analysis of the results, and we are also grateful to Professor Andong Xia at the Institute of Chemistry, Chinese Academy of Sciences, for his fruitful discussions and advice on the time-resolved emission spectroscopy measurement. The reviewers of this paper are specially thanked for their rigorous, inspiring and very helpful comments.

Notes and references

1 T. A. Masters, R. J. Marsh, D. A. Armoogum, N. Nicolaou, B. Larijani and A. J. Bain, *J. Am. Chem. Soc.*, 2013, **135**, 7883–7890.
2 B. Prevo and E. J. G. Peterman, *Chem. Soc. Rev.*, 2014, **43**, 1144–1155.
3 A. K. Woźniak, G. F. Schröder, H. Grubmüller, C. A. M. Seidel and F. Oesterhelt, *Proc. Natl. Acad. Sci. U. S. A.*, 2008, **105**, 18337–18342.
4 T. Ha, X. Zhuang, H. D. Kim, J. W. Orr, J. R. Williamson and S. Chu, *Proc. Natl. Acad. Sci. U. S. A.*, 1999, **96**, 9077–9082.
5 H. Kim, S. C. Abeysirigunawarden, K. Chen, M. Mayerle, K. Ragunathan, Z. Luthey-Schulten, T. Ha and S. A. Woodson, *Nature*, 2014, **506**, 334–338.
6 M. Chien, M. P. Thompson, E. C. Lin and N. C. Gianneschi, *Chem. Sci.*, 2012, **3**, 2690–2694.
7 X. Zhang, S. Rehm, M. M. Safont-Sempere and F. Würthner, *Nat. Chem.*, 2009, **1**, 623–629.
8 J. Y. Shao, H. Y. Sun, H. M. Guo, S. M. Ji, J. Z. Zhao, W. T. Wu, X. L. Yuan, C. L. Zhang and T. D. James, *Chem. Sci.*, 2012, **3**, 1049–1061.
9 R. Abbel, C. Grenier, M. J. Pouderoijen, J. W. Stouwdam, P. E. L. G. Leclère, R. P. Sijbesma, E. W. Meijer and A. P. H. J. Schenning, *J. Am. Chem. Soc.*, 2009, **131**, 833–843.
10 G. McDermott, S. M. Prince, A. A. Freer, A. M. Hawthornthwaite-Lawless, M. Z. Papiz, R. J. Cogdell and N. W. Isaacs, *Nature*, 1995, **374**, 517–521.
11 M. A. Harris, P. S. Parkes-Loach, J. W. Springer, J. B. Jiang, E. C. Martin, P. Qian, J. Y. Jiao, D. M. Niedzwiedzki, C. Kirmaier, J. D. Olsen, D. F. Bocian, D. Holten, C. N. Hunter, J. S. Lindsey and P. A. Loach, *Chem. Sci.*, 2013, **4**, 3924–3933.
12 A. Sautter, B. K. Kaletaş, D. G. Schmid, R. Dobrawa, M. Zimine, G. Jung, I. H. M. van Stokkum, L. D. Cola, R. M. Williams and F. Würthner, *J. Am. Chem. Soc.*, 2005, **127**, 6719–6729.
13 J. A. Riddle, X. Jiang, J. Huffman and D. Lee, *Angew. Chem., Int. Ed.*, 2007, **46**, 7019–7022.
14 B. K. Kaletaş, R. Dobrawa, A. Sautter, F. Würthner, M. Zimine, L. D. Cola and R. M. Williams, *J. Phys. Chem. A*, 2004, **108**, 1900–1909.
15 J. M. Serin, D. W. Brousmiche and J. M. J. Fréchet, *Chem. Commun.*, 2002, 2605–2607.
16 S. Leroy-Lhez, J. Baffreau, L. Perrin, E. Levillain, M. Allain, M. Blesa and P. Hudhomme, *J. Org. Chem.*, 2005, **70**, 6313–6320.
17 G. J. Qi, L. L. Jiang, Y. Y. Zhao, Y. Q. Yang and X. Y. Li, *Phys. Chem. Chem. Phys.*, 2013, **15**, 17342–17353.
18 A. Harriman, G. Izzet and R. Ziessel, *J. Am. Chem. Soc.*, 2006, **128**, 10868–10875.
19 R. T. Cheriya, J. Joy, A. P. Alex, A. Shaji and M. Hariharan, *J. Phys. Chem. C*, 2012, **116**, 12489–12498.
20 R. T. Cheriya, K. Nagarajan and M. Hariharan, *J. Phys. Chem. C*, 2013, **117**, 3240–3248.
21 R. T. Cheriya, A. R. Mallia and M. Hariharan, *Energy Environ. Sci.*, 2014, **7**, 1661–1669.
22 C. Hippius, F. Schlosser, M. O. Vysotsky, V. Böhmer and F. Würthner, *J. Am. Chem. Soc.*, 2006, **128**, 3870–3871.
23 J. R. Lakowicz, *Principles of Fluorescence Spectroscopy*, Springer, Berlin, 2006.
24 R. M. Clegg, *Curr. Opin. Biotechnol.*, 1995, **6**, 103–110.
25 L. Zang, Y. K. Che and J. S. Moore, *Acc. Chem. Res.*, 2008, **41**, 1596–1608.
26 K. R. Wang, D. S. Guo, B. P. Jiang, Z. H. Sun and Y. Liu, *J. Phys. Chem. B*, 2010, **114**, 101–106.
27 A. Datar, K. Balakrishnan and L. Zang, *Chem. Commun.*, 2013, **49**, 6894–6896.
28 F. Würthner, Z. J. Chen, V. Dehm and V. Stepanenko, *Chem. Commun.*, 2006, 1188–1190.
29 Y. K. Che, A. Datar, K. Balakrishnan and L. Zang, *J. Am. Chem. Soc.*, 2007, **129**, 7234–7235.
30 G. Boobalan, P. K. M. Imran, C. Manoharan and S. Nagarajan, *J. Colloid Interface Sci.*, 2013, **393**, 377–383.

31 Y. Liu, Y. J. Li, L. Jiang, H. Y. Gan, H. B. Liu, Y. L. Li, J. P. Zhuang, F. S. Lu and D. B. Zhu, *J. Org. Chem.*, 2004, **69**, 9049–9054.
32 K. Sugiyasu, N. Fujita and S. Shinkai, *Angew. Chem.*, 2004, **116**, 1249–1253.
33 M. R. Islam and P. R. Sundararajan, *Phys. Chem. Chem. Phys.*, 2013, **15**, 21058–21069.
34 A. Wicklein, S. Ghosh, M. Sommer, F. Würthner and M. Thelakkat, *ACS Nano*, 2009, **3**, 1107–1114.
35 A. L. Briseno, S. C. B. Mannsfeld, C. Reese, J. M. Hancock, Y. J. Xiong, S. A. Jenekhe, Z. N. Bao and Y. N. Xia, *Nano Lett.*, 2007, **7**, 2847–2853.
36 E. D. Donato, R. P. Fornari, S. D. Motta, Y. Li, Z. H. Wang and F. Negri, *J. Phys. Chem. B*, 2010, **114**, 5327–5334.
37 B. Yang, F. X. Wang, K. K. Wang, J. H. Yan, Y. Q. Liu and G. B. Pan, *Phys. Chem. Chem. Phys.*, 2014, **16**, 25251–25254.
38 Y. K. Che, X. M. Yang, S. Loser and L. Zang, *Nano Lett.*, 2008, **8**, 2219–2223.
39 Y. K. Che and L. Zang, *Chem. Commun.*, 2009, 5106–5108.
40 Y. Liu, K. R. Wang, D. S. Guo and B. P. Jiang, *Adv. Funct. Mater.*, 2009, **19**, 2230–2235.
41 H. N. Peng, L. P. Ding, T. H. Liu, X. L. Chen, L. Li, S. W. Yin and Y. Fang, *Chem. – Asian J.*, 2012, **7**, 1576–1582.
42 F. Würthner, *Chem. Commun.*, 2004, 1564–1579.
43 X. Zhang, D. Görl and F. Würthner, *Chem. Commun.*, 2013, **49**, 8178–8180.
44 K. Kalyanasundaram and J. K. Thomas, *J. Am. Chem. Soc.*, 1977, **99**, 2039–2044.
45 F. M. Winnik, *Chem. Rev.*, 1993, **93**, 587–614.
46 T. M. Figueira-Duarte and K. Müllen, *Chem. Rev.*, 2011, **111**, 7260–7314.
47 K. Murata, M. Aoki, T. Suzuki, T. Harada, H. Kawabata, T. Komori, F. Ohseto, K. Ueda and S. Shinkai, *J. Am. Chem. Soc.*, 1994, **116**, 6664–6676.
48 Y. C. Lin, B. Kachar and R. G. Weiss, *J. Am. Chem. Soc.*, 1989, **111**, 5542–5551.
49 S. A. Ezzell and C. L. McCormick, *Macromolecules*, 1992, **25**, 1881–1886.
50 K. Balakrishnan, A. Datar, R. Oitker, H. Chen, J. Zuo and L. Zang, *J. Am. Chem. Soc.*, 2005, **127**, 10496–10497.
51 S. Yagai, Y. Monma, N. Kawauchi, T. Karatsu and A. Kitamura, *Org. Lett.*, 2007, **9**, 1137–1140.
52 R. Gvishi, R. Reisfeld and Z. Burshtein, *Chem. Phys. Lett.*, 1993, **213**, 338–344.
53 S. Ando, C. Ramanan, A. Facchetti, M. R. Wasielewski and T. J. Marks, *J. Mater. Chem.*, 2011, **21**, 19049–19057.
54 C. C. You, C. Hippius, M. Grüne and F. Würthner, *Chem. – Eur. J.*, 2006, **12**, 7510–7519.
55 J. G. Vos, R. J. Forster and T. E. Keyes, *Interfacial Supramolecular Assemblies*, John Wiley & Sons Ltd, Chichester, 2003.
56 A. Syamakumari, A. P. H. J. Schenning and E. W. Meijer, *Chem. – Eur. J.*, 2002, **8**, 3353–3361.
57 L. N. Gao, Y. Fang, X. P. Wen, Y. G. Li and D. D. Hu, *J. Phys. Chem. B*, 2004, **108**, 1207–1213.
58 K. Kaushlendra and S. K. Asha, *J. Phys. Chem. B*, 2013, **117**, 11863–11876.
59 X. M. Chang, G. Wang, C. M. Yu, Y. R. Wang, M. X. He, J. Fan and Y. Fang, *J. Photochem. Photobiol., A*, 2015, **298**, 9–16.
60 G. Preti, J. N. Labows, J. G. Kostelc, S. Aldinger and R. Daniele, *J. Chromatogr., Biomed. Appl.*, 1988, **432**, 1–11.